International Journal of Research
Available at https://edupediapublications.org/journals
e-ISSN: 2348-6848
p-ISSN: 2348-795X
Volume 04 Issue 09
August 2017

Modified Sepic Converter and Three-Level NPC Inverter for Reducing Commutation Torque Ripple in BLDC Motor

M. Manoj Ram[1], S. Rahamthulla [2], Dr.P.Sankar Babu[3]
[1]P.G. Scholar, [2]Assistant Professor, [3] Head Of The Department
Branch: Power Electronics
Department : EEE
SVR Engineering College
Email: [1] m.manojram@gmail.com,[2] raham.eee@gmail.com

Abstract:

This paper shows another power converter topology to smother the torque ripple because of the phase current commutation of a brushless dc motor (BLDCM) drive framework. A blend of a three-level diode clasped staggered inverter (3-level DCMLI), an adjusted single-ended primary-inductor converter (SEPIC), and a dc-transport voltage selector circuit is utilized in the proposed torque ripple concealment circuit. For productive concealment of torque pulsation, the dc-transport voltage selector circuit is utilized to apply the directed dc-transport voltage from the adjusted SEPIC amid the commutation interim. So as to additionally moderate the torque ripple pulsation, the 3-level DCMLI is utilized in the proposed circuit. At long last, recreation and experimental results demonstrate that the proposed topology is an alluring alternative to lessen the commutation torque ripple essentially at low-and fast applications..

Keywords: Torque, Commutation, Inverters, Voltage control, Topology, Switches, MOSFET

INTRODUCTION

BRUSHLESS DIRECT CURRENT MOTOR (BLDCM) drives are ending up increasingly mainstream because of its high powerefficiency, high torque to weight and latency proportions, high power thickness, high unique reaction, high dependability, smaller size and basic control. The BLDCMs with trapezoidal back-EMF are utilized broadly in medicinal, aeronautics, electric vehicles, modern and safeguard movement control applications [1]– [3]. Electronically commutated BLDCMs are exceedingly solid and require less upkeep because of the disposal of high-wear parts, for example, standard mechanical commutator and brush get together [4], [5]. In any case, the throbbing torque is one of the key issues in BLDCM. As appeared in Fig. 1, the BLDCM has a trapezoidal back-EMF waveform, and a stator is sustained by semi square wave line current. More often than not, phase winding self-inductance misshapes the perfect semi square wave line current, which makes the torque ripple [4].

Unusual vibration, undesirable speed change, and soundare chiefly created by commutation torque pulsation of BLDCM [6], [7], along these lines, decreasing the torque pulsation is fundamental to enhance the torque execution of the BLDCM drive framework [8]– [15]. The reasons for torque ripple in BLDCM amid commutation interim have been examined for both 120° and 180° electrical conduction methods of the inverter and a composite exchanging mode has been proposed for viable torque ripple concealment at all velocities [8]. In [9], variable information voltage strategy has been proposed for the successful torque

International Journal of Research
Available at https://edupediapublications.org/journals
e-ISSN: 2348-6848
p-ISSN: 2348-795X
Volume 04 Issue 09
August 2017

ripple concealment amid the freewheeling time of BLDCM. In this strategy, the time of the freewheeling area and improved voltage have been assessed utilizing the Laplace change. An epic current control conspire utilizing killjoy current controller has been accounted for the torque ripple decrease of BLDCM utilizing a solitary dc-transport current sensor [10].

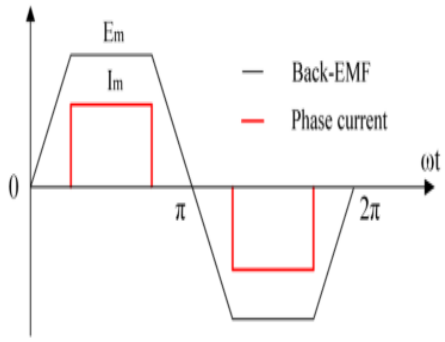

Fig. 1. Ideal back-EMF and current reference waveforms of a single phase.

Different mixture converter topologies have been proposed with a dc-dc converter to enhance torque execution of 2-level inverter-bolstered BLDCM [11]– [14]. In [11], a buck converter has been utilized between the dc supply and ordinary 2-level inverter for the speed control of BLDCM, which can fundamentally lessen the torque ripple at lower speeds. A super-lift Luo-converter has been utilized before the 2-level inverter to lift the dc-transport voltage to the ideal incentive for torque ripple concealment at rapid work conditions [12]. In [13], a novel circuit topology with SEPIC converter and a switch determination circuit has been proposed for torque ripple concealment of BLDCM drive with dc-transport voltage control. To decrease the commutation torque ripple, a voltage control system has been proposed to level theslew rates of approaching and active phase currents. An epic circuit topology has been proposed for torque ripple concealment of BLDCM drive framework which is worked by a 3-level DCMLI with two SEPIC converters and a commutation voltage determination circuit [14]. In [15], a normal torque control strategy utilizing one-cycle control (ATC-OCC) has been proposed utilizing dc-transport voltage and current estimations, without utilizing back-EMF and precise rotor position data. So as to stifle the torque ripple for BLDCM, a current streamlining strategy has been proposed in both conduction mode and commutation mode utilizing necessary variable structure control [16].

In [17], a vector approach has been accounted for the concealment of torque ripple of BLDCM drive by combining the motor current supply. For low inductance BLDCM, a novel torque ripple decrease systems have been proposed dependent on quick torque control approach. A remuneration technique has been created to address the position mistake because of misalignments of magnets and Hall-impact sensors which enhances the exactness of quick torque estimation. Additionally, versatile asymmetry pay work has been created to dispose of an issue related with a voltage unbalance between three phase windings [18], [19]. A cross breed two-and three-phase exchanging mode has been proposed to enhance the torque execution of direct torque controlled BLDCM drive [20]. A direct versatile controller has been proposed to enhance inverter current direction amid extensive back-EMF task, which results in huge torque ripple concealment [21]. An epic current control calculation has been accounted for torque ripple concealment of BLDCM drive utilizing Fourier arrangement coefficients [22].

In most mechanical low-and medium-control applications, a traditional 2-level inverter is a favored decision. The staggered inverter driven air conditioning machines are utilized in numerous modern high power applications because of lower symphonious

mutilation of the yield currents and work with decreased dv/dt worry when contrasted with the 2-level inverter driven air conditioning machines [23]– [25]. The BLDCM is broadly utilized in progressively electric flying machine (MEA) applications in a power scope of 100kW to 150kW and dc-transport voltage is from 270Vdc or 540Vdc. The staggered converters, for example, flying capacitor (FC) inverter, fell H-connect (CHB) inverter, and nonpartisan point-clasped (NPC) inverter have been broadly utilized in high-control medium-voltage applications [26]. For FC inverter, the capacitor clasping requires a substantial number of costly and cumbersome capacitors to clip the voltage. It requires a mind boggling control for voltage following of capacitors, hard to control pre-charging of capacitors to a similar voltage level, and works with poor proficiency. In [27], a 5-level CHB inverter has been proposed for music and torque ripple concealment of BLDCM drive with current and speed shut circle control. This converter needs galvanic partner disconnected dc hotspot for every one of the H-connect. As of late, the MOSFET-based 3-level DCMLIs are wanted to drive BLDCM for low and medium power applications, which create low current THD in the stator windings, littler voltage steps, diminished exchanging misfortune under high exchanging recurrence and lowercommon mode voltage abundancy than customary 2-level inverter [28], [29]. The 3-level DCMLI topology gives a noteworthy decrease in ripple current for low inductance BLDCM without the requirement for high exchanging recurrence than 2-level inverter [30]. Likewise, it works with a lower number of DC sources and power semiconductor gadgets than FC staggered inverter and CHB staggered inverter.

In this paper, a novel converter topology is proposed to diminish the torque ripple of the BLDCM drive framework. The proposed converter is made a changed SEPIC converter and a MOSFET-based 3-level DCMLI. The altered SEPIC converter works with high static gain and less exchanging voltage worry than traditional DC-DC converters [31]. Consequently, the altered SEPIC converter is utilized in this proposed torque ripple concealment circuit and the obligation cycle is changed in accordance with get the ideal dc-transport voltage dependent on the turning pace of the BLDCM. The 3-level DCMLI is utilized for further decrease of the current ripple and also the resultant torque ripple. The MOSFET-based voltage selector circuit is utilized to apply directed dc-transport voltage for proficient commutation torque ripple concealment. Recreation and experimental results demonstrate that the proposed converter topology with the dc-transport voltage selector circuit fundamentally diminishes the torque ripple amid the commutation interim.

BLCD MOTOR

Household appliances are one of the fastest growing markets for BLDCs [1]. Common household appliances which use electric motors include air conditioners, refrigerators, vacuum cleaners, washer sand dryers. These appliances have relied on traditional electric motors such as single phase AC motors including capacitor- start, capacitor-run motors, and universal motors. However, consumers now demand better performance, reduced acoustic noise and higher efficient motor for their appliances. Hence, BLDC have been introduced in order to fulfill these requirements.

Brushless DC motors (BLDC) are usually small horse power control motors that provide various advantages such as high efficiency, quiet operation, high reliability, compact for mandlow maintenance. However, there are disadvantages for the BLDC because of variable speed, and therefore adjustable speed drives are used to overcome this.

BLDC motor applications

Open Loop Applications

Some examples representing open loop control are fans, pumps and blowers. These applications only require a simple low cost controller [1].

2.1.3 Applications with speed control

These applications may demand high speed control accuracy and good dynamic response. Some examples for these applications are washers, dryers and other household appliances. Applications with speed control are also found in the automotive area for uses such as fuel pumps, electronic steering, and engine controls. An advanced control algorithm is often required by these applications, which makes them more expensive [1].

2.1.4 Application with positioning applications

In these applications importance is given to fast dynamic response to speed and torque changes. Many industrial and automation applications come under this category. Also, some of these applications may have frequent reversals of rotational direction. A typical cycle in these applications will consist of four phases: an accelerating phase, a constant speed phase, a deceleration phase and a positioning phase [1].The load on the motor can vary in all these phases, causing an increase in the complexity of the controller's algorithm. These systems mostly operate in closed loop with three control loops functioning simultaneously: a Torque Control Loop, a Speed Control Loop and a Position Control Loop [1]. Sometimes sensors are required to reduce the commutation time.

BLDCs vs. Conventional DC motors

In a conventional(brushed) DC motor, the brushes are responsible for making the mechanical contact with a set of electrical contacts on the rotor referred to as the commutator [1].This forms an electric circuit between the DC electrical source and the armature coil windings. As

The armature rotates the stationary brushes come in contact with different sections of the commutator. The rotating commutator and the brush-system form a set of electrical switches which operate in a sequence to allow electric current to flow through the armature coils closest to the field which may be an electromagnet or a permanent magnet [1].

In a BLDC motor, armature coils do not move, and instead, the permanent magnets rotate. Therefore the armature remains static which avoids the problem of how to transfer current to a moving armature [1].In a BLDC the commutator assembly is replaced by an electronic controller which is programmed to perform the coil switching.

The BLDCs main disadvantage is its cost.

A brief review on control of the BLDC motor

For sensored BLDCs, Hall Effect devices are present in the stator to detect the rotor position. These sensors face the magnets perpendicularly and can distinguish if the North or South Pole is in frontof it. As mentioned earlier, using Hall Sensors in the BLDC can lead to an increase of the overall price of the motor due to an increase in the wiring. Moreover, there are situations where sensors cannot be used in an application such as submersible pumps. In such applications, the sensor lessBLDC control isused. Various control system techniques/ algorithms such as Direct Back EMF zero crossing, Indirect Back EMF Integration and Field Oriented Control (FOC) areused to operatethe motor.

Overview of BLDC Design and Control

BLDC Motor Construction

BLDC motors share some similarities with induction motors and brushed DC motors in terms of construction and working principles. Just like all motors, BLDCs have two important parts: the rotor (rotating part) and the stator (stationary part).

International Journal of Research
Available at https://edupediapublications.org/journals
e-ISSN: 2348-6848
p-ISSN: 2348-795X
Volume 04 Issue 09
August 2017

The stator magnetic circuit is constructed using steel laminations. Steel laminations in the stator can be either slotted (inner rotor design) or slot less (outer rotor design)[14]as shown in Figure2-1.The phase windings are wrapped around the stator, and they can be arranged in two patterns–star (Y)or delta (Δ).The Y pattern gives high torque at low RPM and the Δpattern is used in order to give low torque at low RPM[2].

The rotor of a BLDC is constructed with permanent magnets, and it can consist of various numbers of poles based on the application. Increasing the number of poles gives higher torque but at the cost of reducing the maximum speed. There are two types of BLDC motor designs: Inner and Outer rotor design. In an outer rotor design, the windings are located in the center of the motor and the rotor magnets surround the stator windings. However, the rotor magnets act as an insulator, thereby reducing the rate of heat dissipation from the motor. Due to the location of the stator windings, outer rotor designs typically operate at lower duty cycles or at a lower rated current. The primary advantage of an outer rotor BLDC motor is lower cogging torque [2].

In the inner rotor design, the rotor magnets are surrounded by the stator windings which are affixed to the motor's housing. The primary advantage of an inner rotor construction is its ability to dissipate heat. A motor's ability to dissipate heat also increases its ability to produce torque. For this reason, majority of BLDC motors use an inner rotor design. Another advantage of an inner rotor design is lower rotor inertia [2] which is a factor for speed control.

The BLDC also is referred to as an electronically commuted motor since there are no brushes on the rotor, and commutation is performed electronically at certain rotor positions. Magnetization of the permanent magnets and their displacement on the rotor chosen in such a way that the Back-EMF (the voltage induced into the stator winding due to rotor movement) shape is trapezoidal.Thisallowsarectangular-shaped3-phasevoltage system to be used to create a rotational field with low torque ripple. This differs from Permanent Magnet Synchronous Motor (PMSM) which uses a sinusoidal 3-phasevoltage to create rotational field. PMSMs also have low torque ripple.

The BLDC is usually controlled using a three phase power semiconductor bridge. Control of the bridge requires the rotor position which is obtained using a sensor or a sensor less control technique

Architecture of the BLDC system

The block diagram of a BLDC motor control system is shown in Figure 2-2. The four main parts of the BLDC control system are the power converter, controller, sensors and motor. The power converter is a three phase power semiconductor bridge shown in Figure 2-3.The main function of the power converter is to transform power from the DC source to AC so the motor can convert electrical energy to mechanical energy. The sensor is used to determine the rotor position, and it sends this information to the controller.

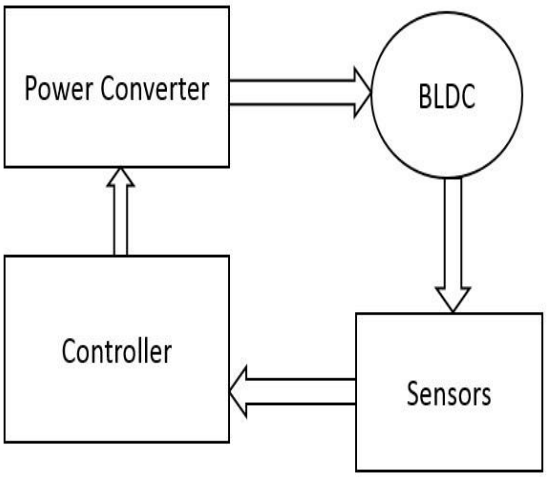

Figure2-2: Block Diagram of BLDC Control[1]

The controller requires feedback information about the rotor position so it can generate a Pulse Width Modulation

(PWM) duty cycle to power the phases of the semiconductor bridge. The controller uses a PWM modulator to generate signals which drive the power converter. The internal block diagram of the power converter and controller is shown in Figure 2-3.

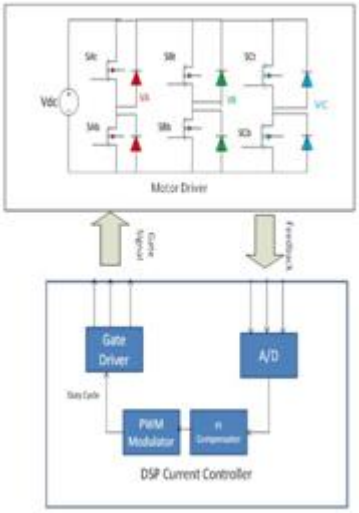

Figure2-3: Internal Block diagram of the Power Converter and Controller[1]

NOVEL TOPOLOGY FOR BLDC MOTOR DRIVE SYSTEM

A system diagram of a proposed new converter topology for BLDCM drive system based on a 3-level DCMLI and a modified SEPIC converter is shown in Fig. 5. In this topology, the 3-level DCMLI is proposed to reduce current ripple, and modified SEPIC converter is included to adjust the dc-bus voltage based on the rotational speed of the BLDCM. The dc-bus voltage- selector circuit is constructed with power MOSFETs (S1, S2, S3, and S4). It is used to select the desired dc-bus voltage for significant torque ripple reduction during commutation interval. The MOSFET-based 3-level DCMLI is operated at a switching of 80 kHz, which provides significant torque ripple suppression than the conventional 2-level inverter. In this 3-level DCMLI, the dc-bus voltage is divided into 3-levels by the capacitors C5 and C6. To obtain the desired commutation voltage, the duty cycle of the modified SEPIC converter can be adjusted during the non-commutation period to maintain Vdc = 8Em. At the start of commutation period, the regulated voltage from the modified SEPIC converter is instantly applied by voltage selector circuit for significant torque ripple suppression.

The commutation path of three-level DCMLI leg A is depicted in the Fig. 6. The following modes of operation of the 3-level DCMLI are discussed based on the polarity of the voltage at the inverter output terminals and direction of the load current.

Operating mode 1: The inverter output voltage, as well as load current (i1) both, are positive. The power MOSFETs QA1, QA2, and clamping diode DM1 are active in this operating mode. The commutation current alternates between the MOSFET QA1 and clamping diode DM1 during the commutation process. The current (i1) flows from the positive terminal of the power supply through the MOSFETs QA1 and QA2 as long as MOSFET QA1 is switched on. If MOSFET QA1 is turned off, load current transfers from MOSFET QA1 to clamping diode DM1. The current now flows from the neutral point (N) to inverter output terminal through the clamping diode DM1 and MOSFET QA2. The MOSFET QA2 remains conducting at all times.

Operating mode 2: In this operating mode, the inverterload current (i1) remains positive but the inverter output voltage is negative. The commutation of current goes back and forth between clamping diode DM1/ MOSFET QA2 and the diodes DA3/DA4.

Operating mode 3: The inverter output voltage, as well as load current (i1) both, are negative. In this operating mode, the commutation current goes back and forth between clamping diode DN1 and MOSFET QA4. When MOSFET QA4 is switched on, the load current (i1) passes

International Journal of Research
Available at https://edupediapublications.org/journals
e-ISSN: 2348-6848
p-ISSN: 2348-795X
Volume 04 Issue 09
August 2017

through MOSFETs QA3 and QA4 from the inverter output terminal. If MOSFET QA4 is turned off, load current transfers from MOSFET QA4 to clamping diode DN1. As a result, the load current now passes through MOSFET QA3 and clamping diode DN1 from the inverter output terminal A to the neutral point (N). The MOSFET QA3 remains conducting at all times.

Operating mode 4: In this operating mode, the inverterload current becomes negative and the output voltage is still positive. The commutation of current goes back and forth between camping diode DN1/MOSFET QA3 and the diodes DA1/DA.

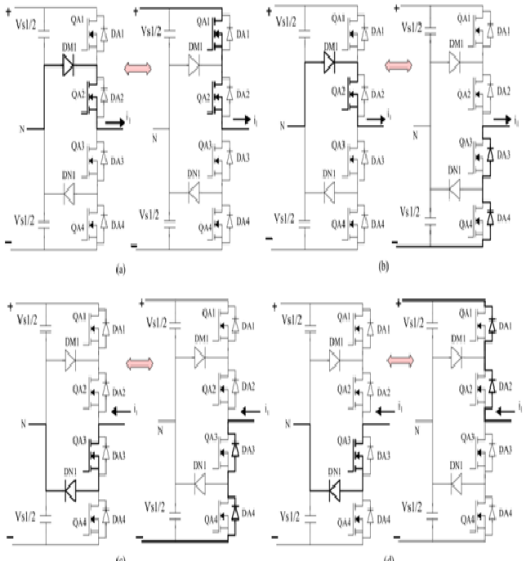

Fig5.1.(a)Operating mode 1,(b) operating mode 2,(c) operating mode 3,(d) operating mode 4.

The mathematical expression for output voltage of the modified SEPIC converter is given as,

$$V_{cv} = \frac{(1+D)V_{s2}}{(1-D)} \qquad (5.1)$$

Where D is the duty-ratio of the modified SEPIC converter. The back-EMF (Em) is proportional to motor speed. i.e.

$$E_m = K_e \omega_m \qquad (5.2)$$

Where, Ke is the back EMF coefficient. The following expression can be used to estimate the duty cycle of MOSFET M based on the measured motor speed.

$$D = \frac{8K_e\omega_m - V_{s2}}{8K_e\omega_m + V_{s2}} \qquad (5.3)$$

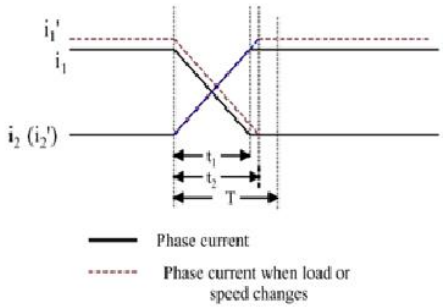

Fig.5.2 phase current changes during commutation period.

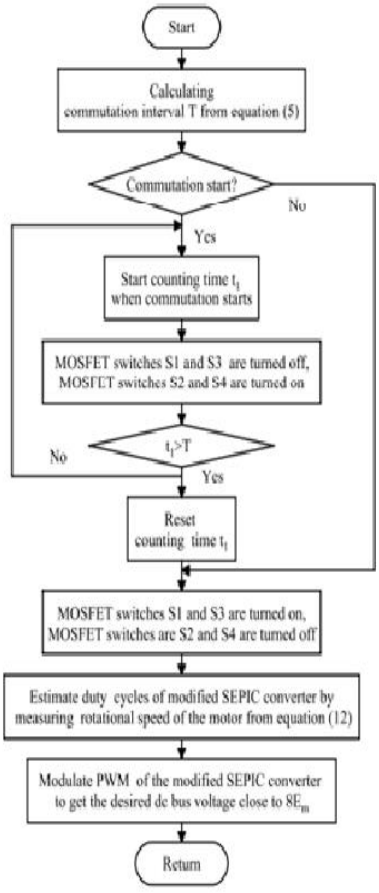

International Journal of Research
Available at https://edupediapublications.org/journals
e-ISSN: 2348-6848
p-ISSN: 2348-795X
Volume 04 Issue 09
August 2017

Fig: 5.3 Flowchart of the proposed voltage control strategy for commutation

Torque ripple suppression

In practice, the commutation period of the BLDCM is much shorter compared to the time taken by the modified SEPIC converter for dc-link voltage adjustment close to 8Em. Hence, MOSFET-based voltage selector circuit has been used, which instantly applies the regulated dc-bus voltage from the modified SEPIC converter for torque ripple suppression during commutation period. Equation (4.5)is used to estimate the real commutation period t1. To compensate load or speed changes, the commutation period T is kept always more than t1and the corresponding relationship is shown in Fig.5.2.This method does not require accurate calculation of commutation period. Fig. 5.4 shows the flow chart ofproposed voltage control method for the proposed topology.

SIMULATION RESULTS

The Mat lab/Simulink model of the BLDCM drive fed with a conventional 2-level inverter, 3-level DCMLI, 2-level inverter with SEPIC converter and a switch selection circuit [13], and the proposed converter are built and simulations are carried out under different switching frequency to investigate the torque ripple pulsation. The simulations are done in the MATLAB/Simulink R2012a software environment. The rated parameters of the BLDCM are listed in Table I. In [13], the SEPIC converter is used to regulate the dc-bus voltage based on the rotational speed of the BLDCM. A dc-link voltage selection and control strategy has been proposed for the commutation torque ripple suppression in BLDCM using MOSFET-based switch selection circuit.

TABLE I
PARAMETERS OF BLDC MOTOR

Rated Voltage (V)	200
Rated Power (W)	518
Rated Speed (r/min)	6000
Rated Torque (N.m)	0.825
Pole Pairs	4
Phase Resistance (Ω)	3.10
Phase Inductance (mH)	3.09
Back-EMF Coefficient (V/(rad/s))	0.227

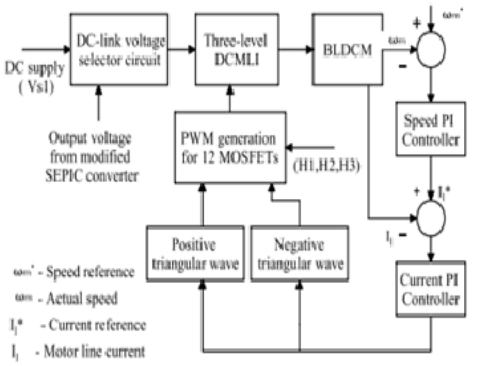

Fig: 6.1.Block diagram of PWM controller for 3-level DCMLI

The control scheme of the 3-level DCMLI, illustrated inFig. 6.1, consists of an outer speed control loop and an inner current control loop. A speed controller that takes inputs fromthe measured speed (ωm) and reference speed (ωm*). The error (ωe) in reference speed and measured speed is amplified by the proportional-integral (PI) controller. The reference current signal generated by the speed controller is compared with the measured current signals and the errors are fed through the PI current controller. The resultant control voltage signals generated by the current controller are compared with positive and negative triangular waveforms to generate PWM signals. Fig.6.2shows the current and torque waveforms when inverters are operated at 5 kHz switching frequency and motor works at 1000 rpm and 0.825 Nm. The result of the same simulation analysis at rated speed is shown in Fig.6.3.Fig.6.4. and Fig.6.5.depict the simulation results at rated torque with 20 kHz switching frequency. Fig.6.4.shows the phase current and torque waveforms at 1000 rpm and

International Journal of Research
Available at https://edupediapublications.org/journals
e-ISSN: 2348-6848
p-ISSN: 2348-795X
Volume 04 Issue 09
August 2017

Fig.6.5.showsphase current and torque waveforms at rated speed.

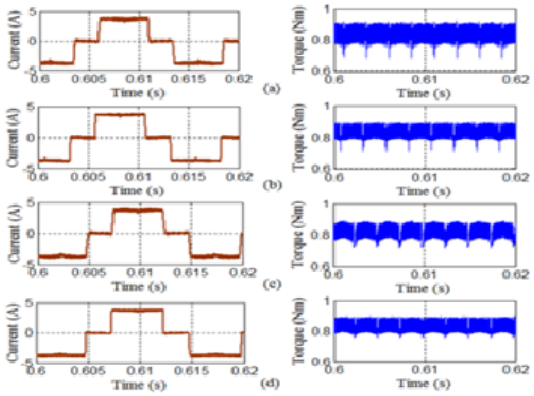

Fig: 6.2.Simulated waveforms of phase current and torque At 1000 rpm and .825 Nm with 5 KHz switching frequency.(a) BLDCM fed by 2-level inverter (b) BLDCM feb by 3-level DCMLI. (C) BLDCM feb by 2-level inverter with SEPIC Converter and a switch selection circuit.(d) BLDCM fed by Proposed topology

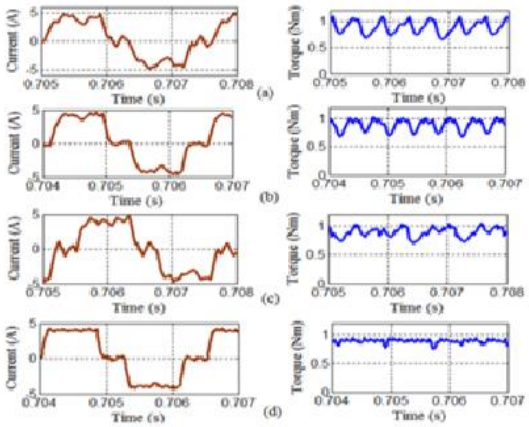

Fig: 6.3.Simulated waveforms of phase current and torque at 6000 Rpm and .825 Nm with 5 KHz switching frequency.(a) BLDCM fed by 2-level inverter (b) BLDCM feb by 3-level DCMLI. (C) BLDCM feb by 2-level inverter with SEPIC Converter and a switch selection circuit.(d) BLDCM fed By Proposed topology

At 80 kHz switching frequency with rated torque, Fig.6.6shows the phase current and torque waveforms at 1000 rpm and Fig.6.7.shows phase current and torque waveforms at rated speed. The comparison of results of these simulation findings clearly shows that the proposed converter topology with dc- bus voltage selector circuit achieves a remarkable reduction in current ripple as well as the commutation torque ripple at low and high speed operations. The regulated dc-bus voltage of 8Em is applied during the commutation interval using dc-bus voltage selector circuit, which results in minimum current ripple and torque ripple. The torque ripple comparison at various speed operations and full load conditions under different switching frequencies of BLDCM fed with two-level, 3-level DCMLI, and the proposed converter topologies are illustrated in Fig.6.8. (a), (b), and (c).

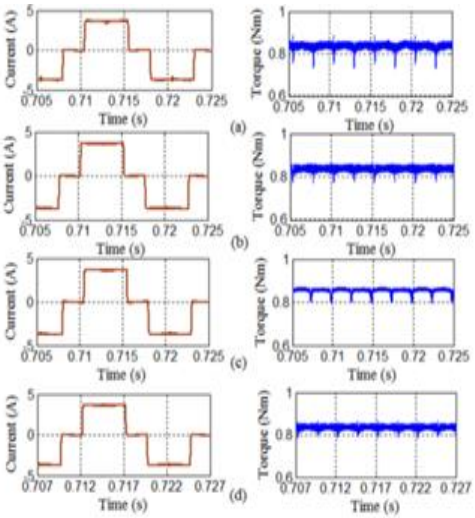

Fig: 6.4.Simulated waveforms of phase current and torqueat 1000 rpm and 825 Nm with 20 KHz switching frequency.(a) BLDCM fed by 2-level inverter (b) BLDCM feb by 3-levelDCMLI. (C) BLDCM feb by 2-level inverter with SEPICConverter and a switch selection circuit.(d) BLDCM fed byProposed topology

International Journal of Research
Available at https://edupediapublications.org/journals
e-ISSN: 2348-6848
p-ISSN: 2348-795X
Volume 04 Issue 09
August 2017

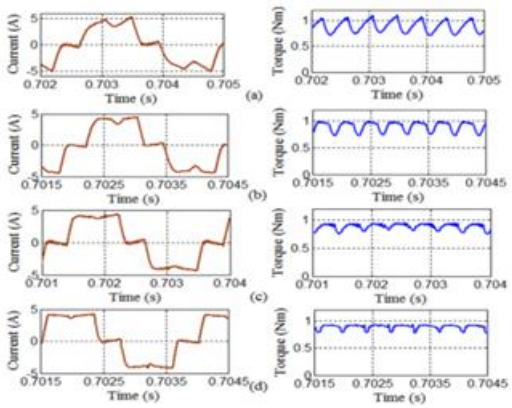

Fig: 6.5.Simulated waveforms of phase current and torque at 6000 rpm and .825 Nm with 20 KHz switching frequency. (a) BLDCM fed by 2-level inverter (b) BLDCM feb by 3-level DCMLI. (C) BLDCM feb by 2-level inverter with SEPIC
Converter and a switch selection circuit.(d) BLDCM fed by Proposed topology

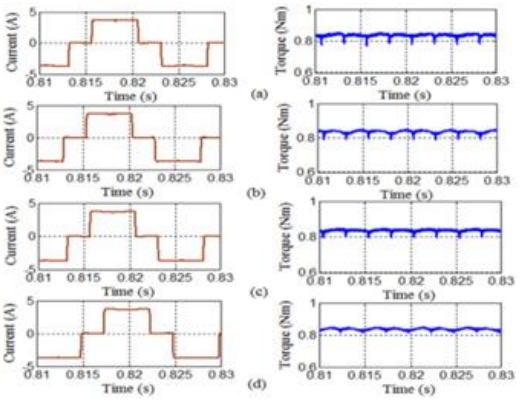

Fig: 6.6.Simulated waveforms of phase current and torque at 1000 rpm and .825 Nm with 80 KHz switching frequency. (a) BLDCM fed by 2-level inverter (b) BLDCM feb by 3-level DCMLI. (C) BLDCM feb by 2-level inverter with SEPICConverter and a switch selection circuit.(d) BLDCM fed by Proposed topology

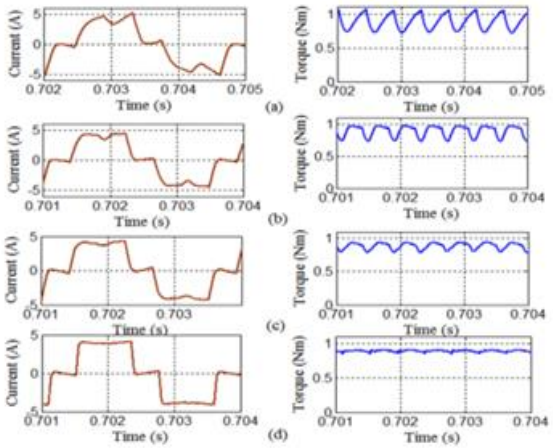

Fig: 6.7.Simulated waveforms of phase current and torque at 6000 rpm and .825 Nm with 20 KHz switching frequency.(a) BLDCM fed by 2-level inverter (b) BLDCM feb by 3-level DCMLI. (C) BLDCM feb by 2-level inverter with SEPIC
Converter and a switch selection circuit.(d) BLDCM fed by Proposed topology

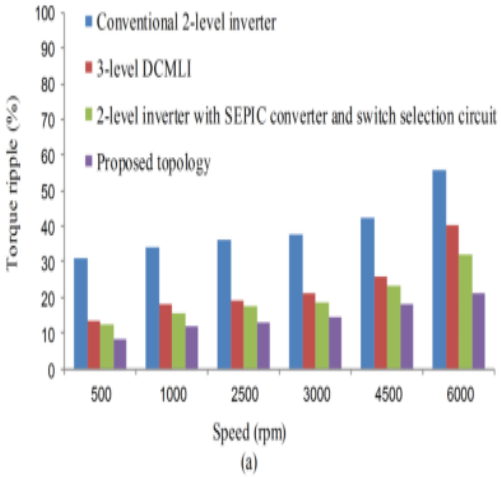

International Journal of Research
Available at https://edupediapublications.org/journals
e-ISSN: 2348-6848
p-ISSN: 2348-795X
Volume 04 Issue 09
August 2017

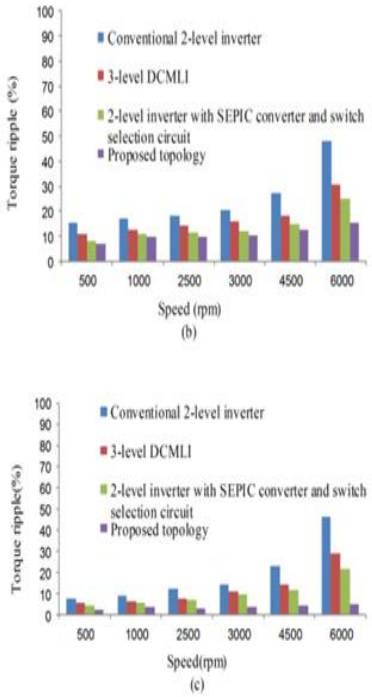

Fig: 6.8. Comparison of the torque ripple for BLDCM fed with 2-level inverter, 3-level DCMLI,2-level inverter with SEPIC converter and a switch selection circuit, and the proposed topology (a) 5KHz switching frequency (b) 20KHz switching frequency (c) 80KHz switching frequency

EXPERIMENTAL RESULTS

Finally, the feasibility and effectiveness of the proposed torque ripple suppression circuit is demonstrated with a BLDCM. The overall converter system schematic and hardware prototype are shown in Fig.17. The control system is employed with SPACE DS1104 control board to implement the proposed control algorithm. To suppress the torque ripple of the BLDCM the 3-level DCMLI is operated at the switching frequency of 80 kHz. In order to determine the rotor position, three Hall-effect sensors are mounted adjacent to the periphery of the rotor. The torque measurement is done by torque sensor FUTEK Modelno.TRS605. The modified SEPIC converter is employed at the entrance of the 3-level DCMLI and operated at 10 kHz switching frequency, which adjusts the duty cycle to get the desired dc-bus voltage based on the measurement of the rotational speed of the BLDCM. The voltage selector circuit applies the desired voltage at the beginning of the commutation to obtain significant torque ripple reduction. The simulation and the experimental results of the BLDCM drive system are in good agreement, which shows the suitability of the proposed converter topology. The proposed topology uses the MOSFET-based dc-bus voltage selector circuit for regulating the dc-bus voltage for effective torque ripple suppression. The duty cycle of the modified SEPIC converter is adjusted to obtain the desired commutation voltage during the non-commutation period to maintain the dc-link voltage equal to 8Em. To select anappropriate dc-bus voltage from Vs1 and modified SEPIC converter, the dc-bus voltage selector circuit uses four power MOSFTEs. The dc-bus voltage (Vdc1) and current waveforms at 6000 rpm are show in Fig.7.2. The waveform for Hall- effect sensor signals at 6000 rpm is shown in Fig.7.3.

The proposed topology is comparatively demonstrated with the conventional 2-level inverter, 3-level DCMLI, and 2- level inverter with SEPIC converter and the switch selection circuit under 5 kHz, 20 kHz, and 80 kHz switching frequencies with the same rating. At rated torque, the experimental results of phase current waveforms and torque waveforms are shown inFigs.7.3-7.8..In table II, the measured torque ripple, calculated total switching loss using analytical equations at various speed operations are compared under different switching frequency. The experimental results show that the proposed converter-fed BLDCM drive operates with the minimum torque ripple than BLDCM fed with the 2-level inverter, 3-level DCMLI, and 2-level inverter with

International Journal of Research
Available at https://edupediapublications.org/journals
e-ISSN: 2348-6848
p-ISSN: 2348-795X
Volume 04 Issue 09
August 2017

SEPIC converter and the switch selection circuit at 80 kHz switching frequency.

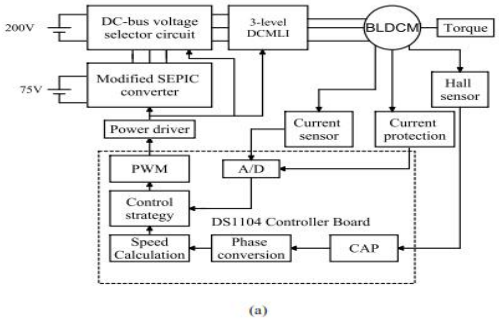

(a)

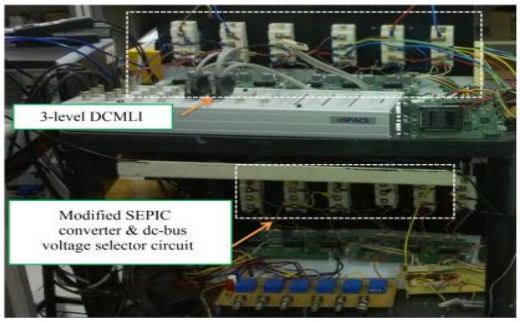

(b)

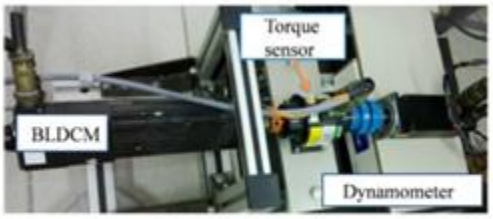

(c)

Fig.7.1.Experimental platform system for torque ripple suppression of BLDCM drive(a) Overall block diagram of the proposed. Torque ripple Suppression circuit with BLDCM (b)3-level DCMLI with modified SEPIC Converter and a dc-bus voltage selector circuit.(c)BLDCM with load Arrangement

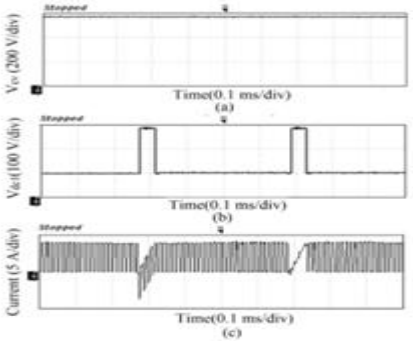

Fig.7.2.Experimental waveforms of the proposed converter at 6000 rpmModified SEPIC converter output voltage (b) dc-bus voltage (V_{DC})(C)DC-bus current

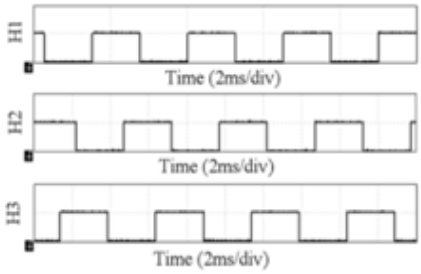

Fig.7.3 Experimental results for Hall-effect sensor signals,HallA,B,AND C at 6000 rpm

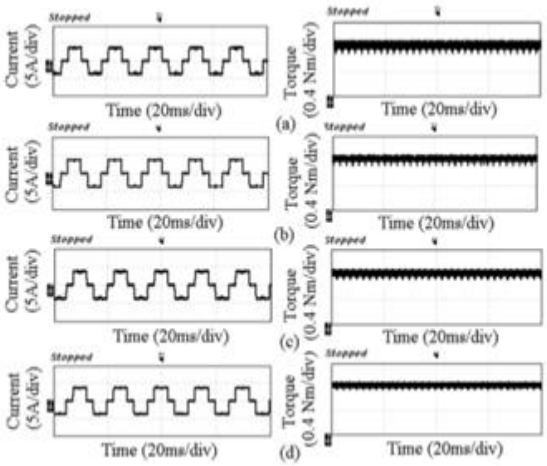

Fig.7.4.Experimental results of current and torque waveforms at 1000 rpm and 0.825 Nm at 5 KHz switching frequency. (a)2-level Fed BLDCM

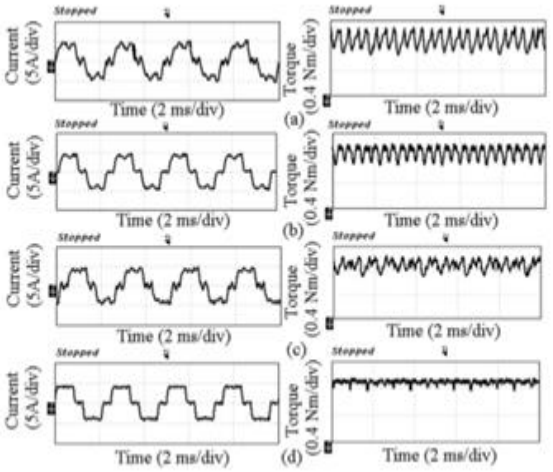

Fig.7.5.Expermental results of current and torque waveforms at 6000 rpm and 0.825 Nm at 5 KHz switching frequency. (a) 2-level Inverter-fed BLDCM drive.(b). 3-

e-ISSN: 2348-6848
p-ISSN: 2348-795X
Volume 04 Issue 09
August 2017

level BLDCM drive (C) 2-level with SEPIC converter and a switch selection circuit-fed BLDCM drive (d). proposed topology-fed BLDCM drive

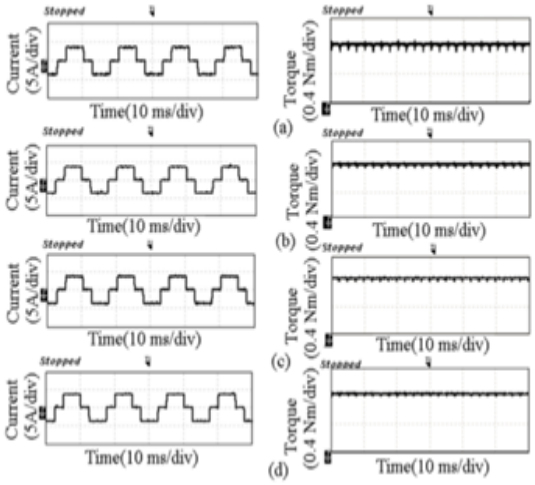

Fig.7.6.Expermental results of current and torque waveforms at 1000 rpm and 0.825 Nm at 20 KHz switching frequency. (a) 2-level Inverter-fed BLDCM drive. (b) 3-level BLDCM drive (C) 2-level with SEPIC converter and a switch selection circuit-fed BLDCM drive (d)Proposed topology-fed BLDCM drive

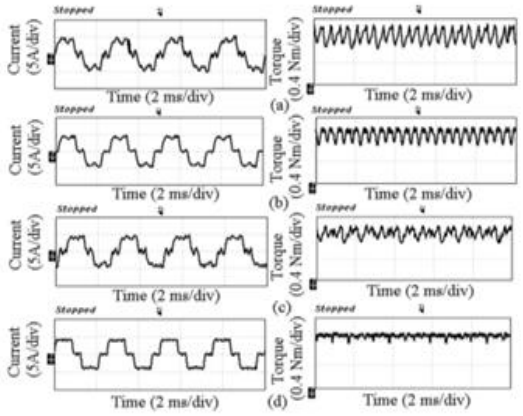

Fig.7.5.Expermental results of current and torque waveforms at 6000 rpm and 0.825 Nm at 5 KHz switching frequency. (a) 2-level Inverter-fed BLDCM drive.(b). 3-level BLDCM drive (C) 2-level with SEPIC converter and a switch selection circuit-fed BLDCM drive (d). proposed topology-fed BLDCM drive

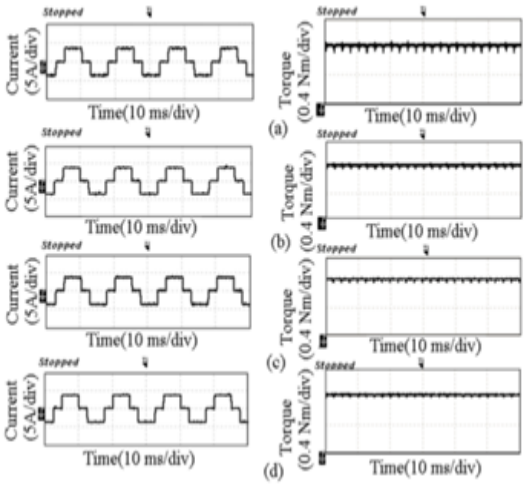

Fig.7.6.Expermental results of current and torque waveforms at 1000 rpm and 0.825 Nm at 20 KHz switching frequency. (a) 2-level Inverter-fed BLDCM drive. (b) 3-level BLDCM drive (C) 2-level with SEPIC converter and a switch selection circuit-fed BLDCM drive (d)Proposed topology-fed BLDCM drive

Fig.7.9.shows the comparison of spectral analysis of torque waveforms generated by the BLDCM drive system at 6000 rpm and 0.825 Nm at 80 kHz switching frequency. It shows the remarkable reduction in the 6th, 12th and 18th harmonics magnitudes by the proposed topology. The total cost of two-level inverter prototype is €293, i.e. €0.293/W. Table III shows the total cost comparison of the 3- level inverter, 2-level inverter with SEPIC converter and the switch selection circuit, and the proposed topology in percentage which is derived from the total cost of 2-level inverter prototype.

International Journal of Research
Available at https://edupediapublications.org/journals
e-ISSN: 2348-6848
p-ISSN: 2348-795X
Volume 04 Issue 09
August 2017

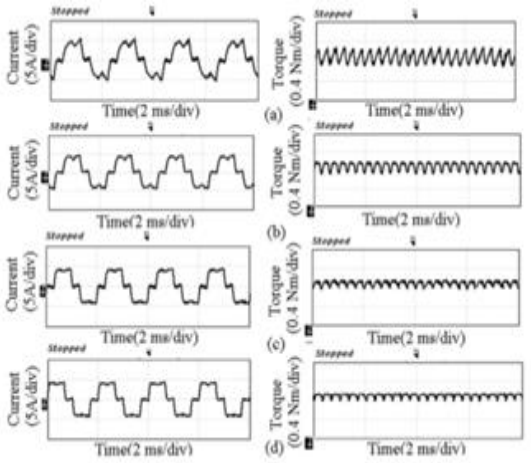

Fig.7.7.Expermental results of current and torque waveforms at 6000 rpm and 0.825 Nm at 20 KHz switching frequency. (a) 2-level Inverter-fed BLDCM drive. (b) 3-level BLDCM drive (C) 2-level with SEPIC converter and a switch selection circuit-fed BLDCM drive (d) Proposed topology-fed BLDCM drive

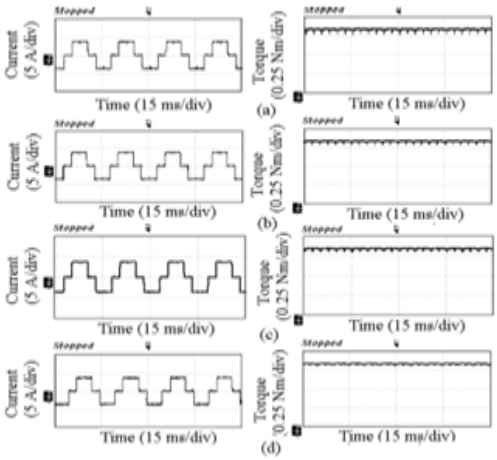

Fig.7.8.Expermental results of current and torque waveforms at1000 rpm and 0.825 Nm at 80 KHz switching frequency.(a) 2-level Inverter-fed BLDCM drive.(b)3-level BLDCM drive (C) 2-level with SEPIC converter and a switch selection circuit-fed BLDCM drive (d)proposed topology-fed BLDCM drive

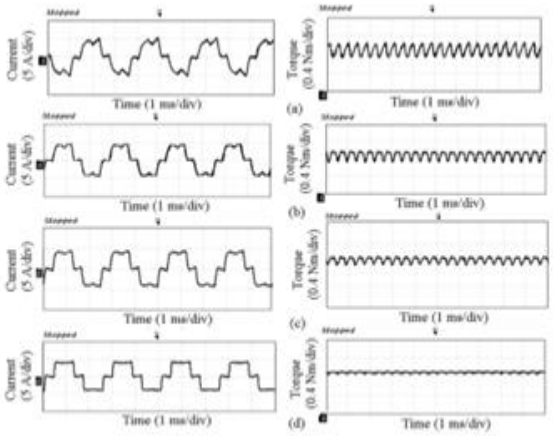

Fig.7.9Expermental results of current and torque waveforms at 6000 rpm and 0.825 Nm at 80 KHz switching frequency. (a) 2-level Inverter-fed BLDCM drive. (b) 3-level BLDCM drive (C) 2-level with SEPIC converter and a switch selection circuit-fed BLDCM drive (d) Proposed topology-fed BLDCM drive

TABLE II
PERFORMANCE COMPARISON

Speed (r/min)	Switching Frequency (kHz)	Torque ripple (%) Load torque =0.825 N.m				Total switching loss (W)			
		2-level inverter	3-level DCMLI	2-level inverter with SEPIC converter and switch selection circuit	Proposed topology	2-level inverter	3-level DCMLI	2-level inverter with SEPIC converter and switch selection circuit	Proposed topology
1000	5	34.7	26.5	22.5	11.9	0.66	0.3	1.3	1.8
	20	17.5	12.4	10.56	9.6	2.7	1.1	3.1	3.3
	80	9.3	6.8	5.8	3.6	12	4.5	13	6.7
6000	5	56.4	47.5	35	21.2	1.4	1.1	5.5	11.6
	20	48.3	39.8	25.1	15.4	6	5	10.3	15.5
	80	46.4	40.3	21.4	5.1	39	19	46	28.6

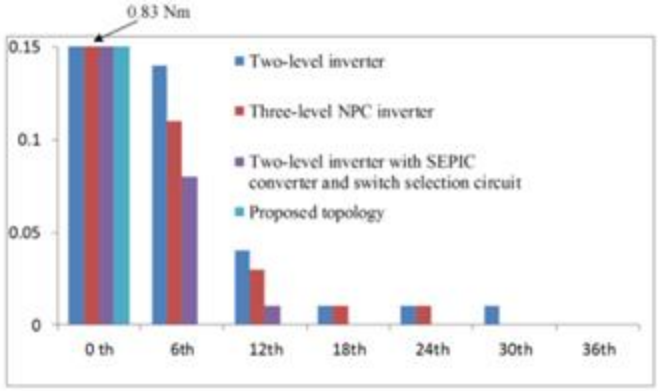

TABLE III
COMPARISON OF INVERTER'S COSTS

Cost comparison (%)			
2-level inverter	3-level DCMLI	2-level inverter with SEPIC converter and switch selection circuit	Proposed topology
100	136	157	189

From Table III it is seen that the proposed topology has the highest cost due to clamping diodes of DCMLI and modified SEPIC converter; however, the torque ripple is substantially reduced by the proposed topology at the higher operating speed. Furthermore, it operates with lower switching losses than the 2-level inverter and 2-level inverter with SEPIC converter and switch selection circuit fed BLDCM drive system at 80 kHz switching frequency.

CONCLUSION

In this paper, a commutation torque ripple decrease circuit has been proposed utilizing 3-level DCMLI with changed SEPIC converter and a dc-transport voltage selector circuit. A research facility fabricated drive framework has been tried to check the proposed converter topology. The recommended dc-transport voltage control procedure is progressively powerful in torque ripple decrease in the commutation interim. The proposed topology achieves the effective decrease of torque ripple in the commutation time frame and experimental results are introduced to think about the execution of the proposed control system with the regular 2-level inverter, 3-level DCMLI, 2-level inverter with SEPIC converter and the switch determination circuit-bolstered BLDCM. So as to acquire critical torque ripple concealment, quietness and higher productivity, 3-level DCMLI with changed SEPIC converter and the voltage selector circuit is a most appropriate decision to get elite task of BLDCM. The proposed topology might be utilized for the torque ripple concealment of BLDCM with the plain low stator winding inductance.References

1. N. Milivojevic, M. Krishnamurthy, Y. Gurkaynak, A. Sathyan, Y.-J. Lee, and A. Emadi, "Stability analysis of FPGA-based control of brushless DC motors and generators using digital PWM technique," IEEE Trans. Ind. Electron., vol. 59, no. 1, pp. 343–351, Jan. 2012.
2. X. Huang, A. Goodman, C. Gerada, Y. Fang, and Q. Lu, "A single sided matrix converter drive for a brushless dc motor in aerospace applications," IEEE Trans. Ind. Electron., vol. 59, no. 9, pp. 3542–3552, Sep. 2012.
3. X. Huang, A. Goodman, C. Gerada, Y. Fang, and Q. Lu, "Design of a five-phase brushless DC motor for a safety critical aerospace application," IEEE Trans. Ind. Electron., vol. 59, no. 9, pp. 3532-3541, Sep. 2012.
4. J.-G. Lee, C.-S. Park, J.-J. Lee, G. H. Lee, H.-I. Cho, and J.-P. Hong, "Characteristic analysis of brushless motor condering drive type," KIEE, pp. 589-591, Jul. 2002.
5. T. H. Kim and M. Ehsani, "Sensorless control of BLDC motors from near-zero to high speeds," IEEE Trans. Power Electron., vol. 19, no. 6, pp. 1635–1645, Nov. 2004.
6. T. J. E. Miller, Switched Reluctance Motor and Their Control. London, U.K.: Clarendon, 1993.
7. K. Ilhwan, N.Nobuaki, K.Sungsoo, P.Chanwon, and Chansu Yu, "Compensation of torque ripple in high performance BLDC motor drives," Control Eng. Pract., vol.18, pp. 1166-1172, Oct. 2010.
8. S. S. Bharatkar, R. Yanamshetti, D. Chatterjee, and A. K. Ganguli, "Reduction of commutation torque ripple in a brushless dc motor drive," in Proc. IEEE PECon, 2008, pp. 289–294.

9. K.-Y. Nam, W.-T. Lee, C.-M. Lee and J.-P. Hong, "Reducing torque ripple of brushless DC motor by varying input voltage," IEEE Trans. Magn., vol. 42, no. 4, pp. 1307–1310, Apr. 2006.
10. [10] J. H. Song and I. Choy, "Commutation torque reduction in brushless DC motor drives using a single DC current sensor," IEEE Trans. Power Electron. vol. 19, no. 2, pp. 312–319, Mar. 2004.
11. [11] X. F. Zhang and Z. Y. Lu, "A new BLDC motor drives method based on BUCK converter for torque ripple reduction," Proc. IEEE Power Electron. Motion Control Conf., 2006, pp. 1-4.
12. [12] W. Chen, C. Xia, and M. Xue, "A torque ripple suppression circuit for brushless DC motors based on power DC/DC converters," in Proc. IEEE Ind. Electron. Appl. Conf., 2008, pp. 1453–1457.
13. [13] T. Shi, Y. Guo, P. Song, and C. Xia, "A new approach of minimizing commutation torque ripple for brushless DC motor based on DC–DC converter," IEEE Trans. Ind. Electron., vol. 57, no. 10, pp. 3483–3490, Oct. 2010.
14. [14] V. Viswanathan and S. Jeevananthan, "Approach for torque ripple reduction for brushless dc motor based on three-level neutral-point-clamped inverter with dc-dc converter," IET Power Electronics, vol. 8, no. 1, pp. 47-55, 2014.
15. [15] T. Sheng, X. Wang, J. Zhang, and Z. Deng, "Torque-Ripple mitigation for brushless DC machine drive system using one-cycle average torque control," IEEE Trans. Ind. Electron., vol. 62, no. 4, pp. 2114-2122, Apr. 2015.
16. [16] C. Xia, Y. Xiao, W. Chen, and T. Shi, "Torque ripple reduction in brushless DC drives based on reference current optimization using integral variable structure control," IEEE Trans. Ind. Electron., vol. 61, no. 2, pp. 738–752, Feb. 2014.
17. [17] G. Buja, M. Bertoluzzo, and R. K. Keshri, "Torque ripple-free operation of PM BLDC drives with petal-wave current supply," IEEE Trans. Ind. Electron., vol. 62, no. 7, pp. 4034–4043, Jul. 2015.
18. [18] J. Fang, X. Zhou and G. Liu, "Instantaneous torque control of small inductance brushless DC motor," IEEE Trans. Power Electron., vol. 27, no. 12, pp. 4952–4964, Dec. 2012.
19. [19] J. Fang, X. Zhou and G. Liu, "Precise accelerated torque control for small inductance brushless DC motor," IEEE Trans. Power Electron., vol. 28, no. 3, pp. 1400-1412, Mar. 2013.

[20] Y. Liu, Z. Q. Zhu, and D. Howe, "Instantaneous torque estimation in sensorless direct-torque-controlled brushless DC motors," IEEE Trans. Ind. Appl., vol. 42, no. 5, pp. 1275–1283, Sep./Oct. 2006